A Multi-Channel Electrode for Chronic Recording and Safe Current-Steered Stimulation

Ben Pearre[1,a,¤], Sanne Moorman[1,b], Jun S. Song[1,c], Timothy J. Gardner[1,d]

[1] Department of Biology, Boston University, Boston, Massachusetts, United States of America

Author [a] contributed the original Matlab and LabView implementations and most of the manuscript. Author [b] performed the surgeries and histologies.

[¤] Corresponding author: bwpearre@gmail.com (BP)

Abstract

Long-term recording enables.... stimulation enables...

Big electrodes — effective for low-voltage stimulation, but damage going in, gliosis on timescales like a month.

Current steering — dbs: no learning control. "Adaptive" dbs, model-based coarse-grained current steering.

Small electrodes (under 10 mm) cause less acute and chronic damage, but are delicate. We have developed an electrode design in which groups of electrodes support each other during insertion.

We show that the bundled electrodes splay in the brain.

We present preliminary results showing that these electrodes can remain capable of recording individual spikes for a year after implantation, even when also used to stimulate.

We present preliminary evidence that the spatial scale of the splaying is sufficient to allow the steering of current between the electrodes, and that this allows some degree of high-dimensional control over the brain's response to stimulation.

1 Introduction

1.1 Review of current steering

Much of the work in current steering in the brain is due to the interest in deep brain stimulation (DBS). Electrodes tend to be single rods 1.2–1.6 mm in diameter with 4–32 contacts.

DBS has been used to treat movement disorders (Parkinson's disease), epilepsy, Alzheimer's, chronic pain, cluster headache, depression, OCD, addictive behaviours, anorexia...

Many more! But do we want to provide a big list? Only if we are selling this as a clinical paper, right?

Most attempts to steer current use computational models of brain tissue to predict current-steering configurations that preferentially target the intended type of tissue, or make up for errors in electrode placement during surgery [1]. Macroscopic models, with voxels of 1–2 mm^3: [2] uses 3D finite element analysis to predict current steering trajectory. They built a model based on magnetic resonance imaging (MRI) and diffusion tensor imaging (DTI) [3], which produces data with voxels of roughly 2 mm^3.

Verification??

Lots more references might be added here, all of which have spatial resolution on this order and a variety of temporal resolutions; choose ≈3 or just cite a review?

Current steering on a smaller scale: [4] use 64-channel electrode arrays, with electrode as closely packed as 30 μm, to stimulate macaque retina *in vitro*. They stimulated the retina using single electrodes or combinations of three electrodes with charge-balanced pulses, and found that retinal response could be predicted with a piecewise linear model.

Note about how different retina structure is from our areas?

1.2 Stimulation: closing the loop

Standard DBS systems deliver some kind of stimulation continuously. Recently, interest in using biological feedback has grown. Due to the size of the electrodes, for feedback control most systems rely on large-spatial-scale metrics such as local field potentials (LFP) [5] and other macroscopic measures of outcome such as accelerometers [6], but the addition of a second electrode in a different brain region has been shown to be effective in ameliorating Parkinsonian symptoms in monkeys [7].

1.3 Review of electrode size and damage

Large electrodes must be stimulated at high currents. Energy inefficiency. Imprecision. Sense-act cycles are limited.

Electrodes with cross-sectional dimension above about 10 μm result in glial scarring up to 300 μm from the implant, tissue damage, ever-increasing stimulation thresholds, unable to record from some cell types [8, 9].

Charge injection In order to increase the charge injection capacity of our electrodes, we tried electroplating them with iridium oxide. This effected an improvement of roughly an order of magnitude: impedances went from around 2 MΩ to 200 kΩ, and for a given current, the required voltage was much lower. We also experimented with PEDOT, which has excellent charge-injection properties, but we found it to have durability issues. See [10] for a review of electrode physics.

FIXME

All I know about this is hearsay.

2 Materials and Methods

2.1 Bird surgery description

Jun?

Ground/return electrode should be described somewhere. Here?

2.2 Electrode construction

Electrode arrays were constructed as described in [11]. The charge transfer capacity of one of the stimulation electrodes was enhanced by electrodeposited iridium oxide. [10] describes the electrochemistry of charge transfer.

2.3 Splay histology

Electrode bundles were implanted into birds, all to a depth of roughly 3 mm. Most of these were "dummy" uncoated and blunt-cut rather than fire-sharpened as in [11], with 10–16 channels (fibres). The birds were killed, and their brains sectioned roughly perpendicularly to the electrodes, with a slice thickness of 50 μm.

Sanne: what slice thickness?

The following criteria were used to exclude observations:

Sanne: check exclusion criteria.

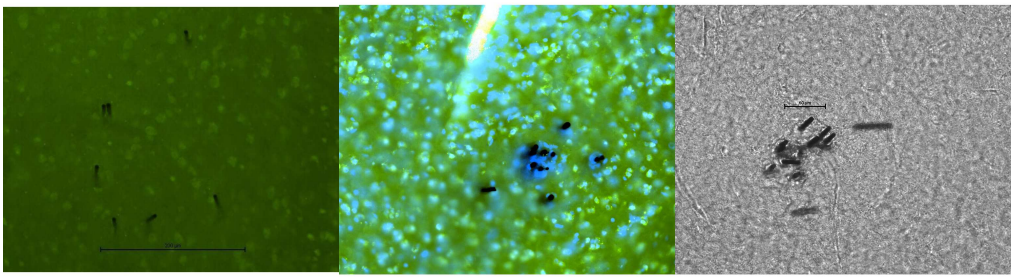

Figure 1. Splay types, left to right: examples of full splay, partial splay, and clumped. In all images, black circles are electrode shafts; in many cases the slicing plane is not quite orthogonal to the electrodes, yielding oblong images. In the bright-field image on the right, three of the electrode slices were pulled out of the tissue during slicing, and appear to lie flat on the slide. Since their original locations cannot be determined, we have ignored them.

- Individual fibres were excluded if they were lying flat on the surface of the tissue (visible as side-on cylinders).
- Bundles were excluded if they were implanted in fibres of passage.

Clustering was done by hand. The set of distances between electrodes was computed by measuring the distance between each electrode and its nearest neighbour. Bundles were clustered as follows:

I'm about a day from finishing software to do all-to-all comparison. For the draft (and possibly first submission, if time is tight) this suffices.

Splayed: All electrodes were more than 10 μm from each other, or at most one pair was closer.

Why 10 μm?

How many?

Partial: Some electrodes were more than 10 μm from each other.

All-to-all, or nearest-neighbour?

Clumped: All electrodes were within 10 μm of each other.

Would it make sense to automatically cluster the splay data? Or to change the criteria? I can think of some changes...

Examples of these three categories are shown in Fig. 1.

2.4 Recording

Recordings of spontaneous activity were done using an Intan RHD2000 amplifier at 20 kHz, with a hardware high-pass filter at 200 Hz.

2.5 Stimulation: Zebra finch antidromic HVC ← X

A common technique for locating HVC in the zebra finch involves implanting a stimulating electrode in Area X and looking for a an antidromic response [12, 13],

which is visible in HVC but not in the surrounding tissue.

Electrical stimulation saturates the brain, including the recording electrode, for some time post-stimulation (depending on the hardware used, but generally 1–3 ms post-stimulation). Responses to stimulation can be detected outside of that saturation window.

We tested our ability to steer current in the brain by stimulating in Area X and monitoring the response in HVC, about 5 mm away. This spatial separation results in synaptic transmission delays of between 3 and 8 ms , which gives the recording amplifier time to settle before measuring the response.

Tim: citation for 3–8 ms?

But why antidromic?

We will use the following definitions:

Channel: Our electrodes have 16 separate carbon fibres, each one of which we consider a separate channel, since each is connected to a separate amplifier. Some work better than others, and usually about 75% of them have low enough impedance to use. We refer to these as active channels, or just channels.

Pulse: A biphasic charge-balanced square wave of current. Each phase is 200 μs long, and there is no interpulse interval.

Current-steering configuration (CSC): The configuration defining which channels receive the positive half of their biphasic pulse first, or vice versa.

Pulse train: A sequence of 10 identical pulses delivered simultaneously to all active chennels at 25 Hz. This is slow enough that pulses do not interfere with each other, and is used to detect the reliability of the response.

- Programming the Plexon stimulator for one pulse train requires about 2 seconds.

Move timing notes to Discussion of compromises required for this experiment?

Threshold scan: A series of pulse trains, each of which has the same CSC but a different current, designed to find the minimum current for this CSC that will antidromically induce a response in HVC. The algorithm is described below.

- A threshold scan generally requires roughly 15 pulse trains, and thus takes on the order of 30 seconds.

Voltage scan: The Plexon hardware can deliver a current-controlled pulse to each of 16 channels independently, but only allows monitoring of the voltage delivered on one channel at a time. A voltage scan involves sending the same pulse train once per active electrode, monitoring a different one each time.

This does not require full reprogramming of the Plexon! Just setting the monitor channel is faster, but my code does not take advantage of this, and fully reprogrammes the Plexon each time.

- A voltage scan requires delivering one pulse train per active electrode, taking a total of about 30 seconds.

The stimulation and recording electrodes use separate electrical returns, consisting of silver wire in contact with the skull. Some CSCs balance current delivery between the electrodes, whereas others do not, and in the latter case excess current flows through the common return.

Jun?

We used a Plexon stimulator to control stimulation in Area X, and recorded from HVC using a Tucker-Davis Technologies RZ5 amplifier. The Plexon self-monitoring channels were recorded on a National Instruments PCI-6251 data acquisition card using the session-based interface of Matlab (various versions from 2014a through 2015b) on Windows 8.1.

And/or an Intan, depending on which recording to show in Fig. 2

We used MATLAB to control the stimulation and acquisition as follows: the National Instruments card is set to record an adequate number of samples of the Plexon self-monitoring channels at 100 kHz, initiated through software, and sending out a TTL pulse at the beginning of acquisition. The Plexon stimulator begins stimulating upon receipt of that TTL pulse, and the TDT begins recording at 24.414 kHz (the device's native frequency) on the same signal. Whenever the Plexon is actively delivering current (i.e. during each pulse within the train) it sends out its own TTL pulse: this signal is recorded by the TDT along with the HVC electrode voltages in order to align stimulation pulses with the recording. The alignment precision is limited only by the sampling rate of the TDT.

Response detection HVC projects into Area X (and into RA, which we do not discuss here). When Area X is stimulated, an antidromic response may be observed both in HVC_X projection neurons and in HVC interneurons. The antidromic response occurs roughly 3–8 ms after the stimulation pulse, and is highly stereotyped: [14] reports that the variability in the timing of the antidromic response in HVC_X

Citation!

projection neurons is under 50 μs, while that of HVC intraneurons is above 500 μs.

Fig. 2 shows an example of a pronounced HVC response to stimulation in Area X. In order to detect this signal, we measure the cross-correlation between the recorded response for each pulse in a train and each other with a maximum lag of 50 μs, which provides a robust way of separating neural response from noise. Because the HVC amplifier's response to the transient stimulation pulse in Area X can persist into the time of interest (3–8 ms), each response is first de-trended using a maximum-likelihood fit over the region 2–25 ms using an eigth order Fourier Series, which removes post-stimulation decay while leaving intact spike-sized signals. We found this to produce fewer artifacts than the more conventional approach of bandpass-filtering the signal, given the large stimulation artifact. The cross-correlation threshold above which a response is identified is chosen by visual inspection.

Filtering would probably work better with the TDT...

As the bird ages, the skull grows down from the implantation site. For shallow installations such as HVC (depth $\approx 200\mu m$, the quality of the HVC recordings diminishes as electrodes are forced out of contact with the brain. This makes it more and more difficult over time to measure the antidromic response. The above cross-correlation technique is more sensitive than the technique typical of acute or short-term response measurements, in which a pronounced spike is often clearly visible. We believe that we are measuring an antidromic response because it is on the correct timescale and appears near the expected stimulation threshold.

But now why not findpeaks 3σ or whatever, and see if peak jitter is $< 50\mu$s as required by [14]? This has the great advantage that over an n-spike train, I could immediately compute Pr(response) (see marginpar QWE to see why this is a good idea). Could re-analyse old data this way and compare, and decide whether to go forward.

Need to prevent antidromic response transmission and see if "measured response" disappears as it should! But this requires more birds, and a more complex experiment.

Cite papers giving timing and stimulation threshold.

Threshold scan What stimulation parameters are required in order to reliably elicit an antidromic response to stimulation in Area X? How can this threshold be found quickly, while minimising the risk of exceeding safe stimulation voltages? How can this process be made robust to noise?

How can we establish how much robustness to noise is required?

Perhaps write a pseudocode block instead of this mess?

After choosing a CSC, we begin stimulating at a current that is known to be below threshold. While no response is seen, the current is increased gradually (by a factor of $\alpha \approx 1.1$) until either a response is detected or the voltage or current limit is exceeded. In the latter case, a lack of response is reported, and we move on to the next CSC. If a response is found, then the step size is decreased ($\alpha \leftarrow \alpha^{2/3}$) and we reduce the current until the response disappears. This process is repeated until the step size drops below a limt ($\alpha < 1.02$), and the threshold is taken as the last parameter set

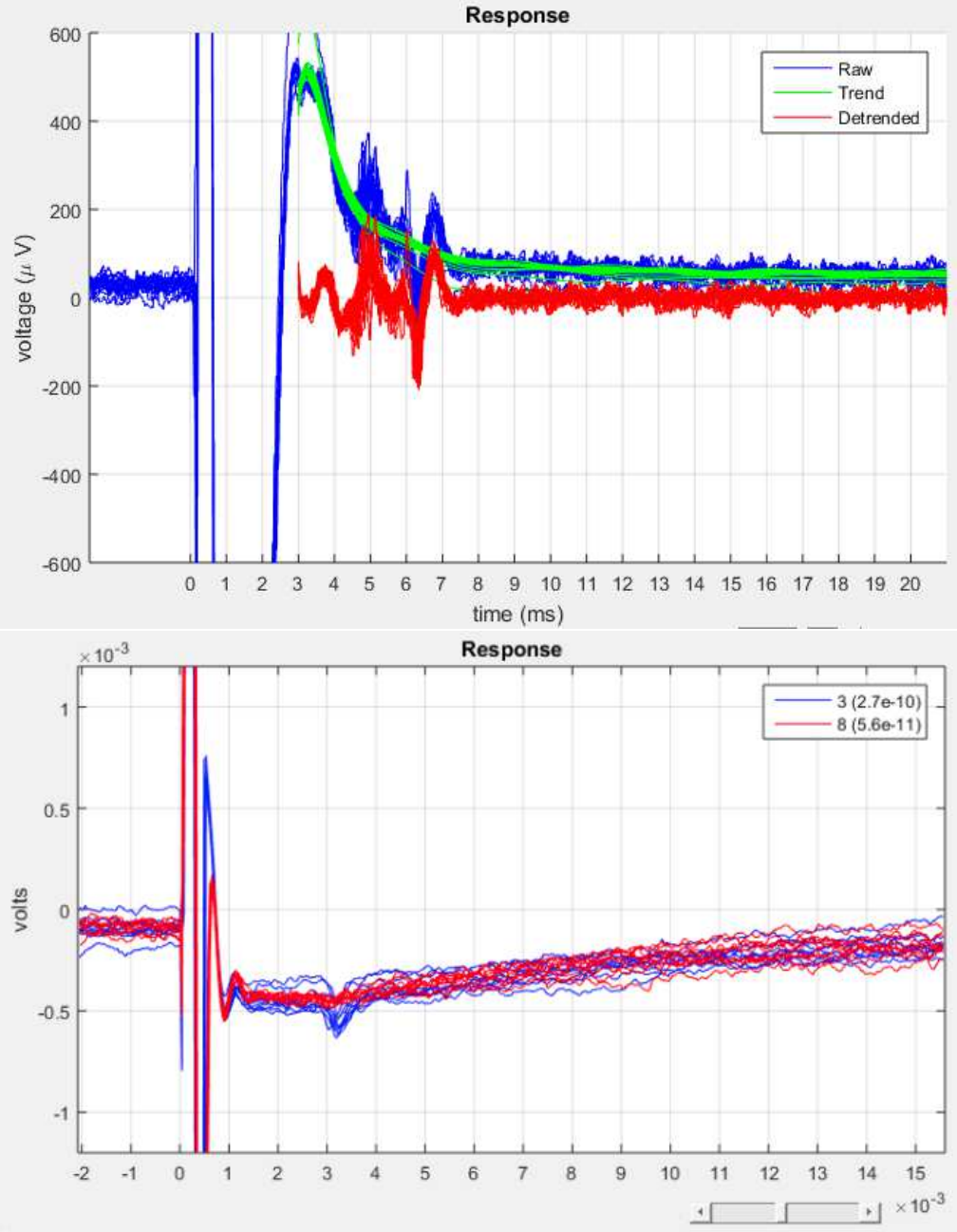

Figure 2. An example of a strong response in HVC. **Top:** The horizontal axis is time in milliseconds relative to the onset of a stimulation pulse. Here, the stimulation is a 400-μs biphasic pulse of 3 μA, in which voltage peaked at 1.6 V. Stimulation was repeated 20 times at 25 Hz, with each response aligned to its respective pulse. Various response activity can be seen, but the most pronounced is at 6.2 ms post-onset. **Bottom:** a different bird, with a much weaker signal, but recorded on TDT. 200 μs, 6.94 μA, 1.2 V peak. *Use the top figure? It only shows one channel, and it's recorded on the Intan, which I was using while the HVC signals were still pretty. That means a lot worse amplifier settling, so it's not the best image, but the response is much cleaner than later ones made with the TDT.*

QWE: This was expedient, but is primitive! I had planned to use all the data as follows: during threshold scan and during voltage scan, sweep around area of interest, find Pr(response | . . .), fit a sigmoid to this curve, and take e.g. midpoint or etc. Search could even be conducted as above (although could do better) or terminated by estimating the error on the estimate. I can almost certainly get better results by re-analysing the old data this way.

that induced a response.

While a larger step size would result in a faster search, and a binary search would be easier to describe, this ad-hoc approach samples near the current of interest while making it unlikely that we will stimulate with a current that significantly exceeds the minimum required for a response.

Voltage scan Once the minimum current required in order to achieve a response is identified, we perform a voltage scan at that current, in order to measure the peak voltage delivered to each electrode.

3 Results

3.1 Splay histology

After exclusion, 22 arrays, implanted into 13 different birds, each yielded at least 3 measurable electrodes. See Table 1 for the raw data and Fig. 3 for visualisations thereof.

Perhaps take out the table and just use the graphs?

Fig. 4 shows some examples of the damage done to the brain in the vicinity of tle electrodes. Visual inspection shows little damage in the vicinity of single electrodes, and slightly more in clumped electrode groups. Visual inspection can give some indication of the damage done to the brain and the likelihood of achieving good electrical contact with neurons, but we are more interested in the ability to record signals (see Section 3.2).

An image of "typical" damage done by "micro"electrodes would be nice, but it's hard to show what's typical of the ~~competition~~ prior work with any credibility. Letting people compare vs. their own experiences is the best, but not everyone (e.g. me) will know what's typical.

I have data on how long post-implant the birds lived, which needs to come along with this figure, if not the rest of the paper.

3.2 Chronic recording

Need a graph showing impedances per electrode over time. At least I have data for that; just haven't writtent the code to extract+plot.

Impedances

HVC Long-term recording in HVC is difficult due to skull regrowth interfering with electrodes implanted only a few hundred microns from the surface: after 10 months, we had difficulty picking up antidromic response in our two remaining birds.

Area X More telling of the potential of these electrodes is the recording of spontaneous activity in Area X, which was still easily seen in several channels after a

	Inter-electrode distance (μm)		
# Good electrodes	Mean	StdDev	Max
3	5.0	0	20.0
10	6.0	2.1	52.9
16	6.3	6.3	48.3
4	7.5	5.0	35.8
6	16.7	18.9	44.8
9	7.7	5.5	107
14	12.8	12.1	15.2
8	14.7	17.8	108
15	15.1	10.2	163
15	19.3	19.1	128
5	22.0	27.7	103
9	28.2	35.8	148
11	31.8	28.1	103
8	35.9	30.6	228
13	76.5	152	167
5	51.4	28.1	51.5
3	20.0	0	123
6	73.5	35.5	128
8	38.5	35.2	142
9	47.4	31.5	208
5	126	63.5	214
16	62.0	58.9	829

Table 1. Raw data. Each row shows the statistics from one electrode array. "Good" electrodes is the the number of carbon fibre electrodes in each bundle that appeared to still be firmly fixed in the neural tissue after slicing.

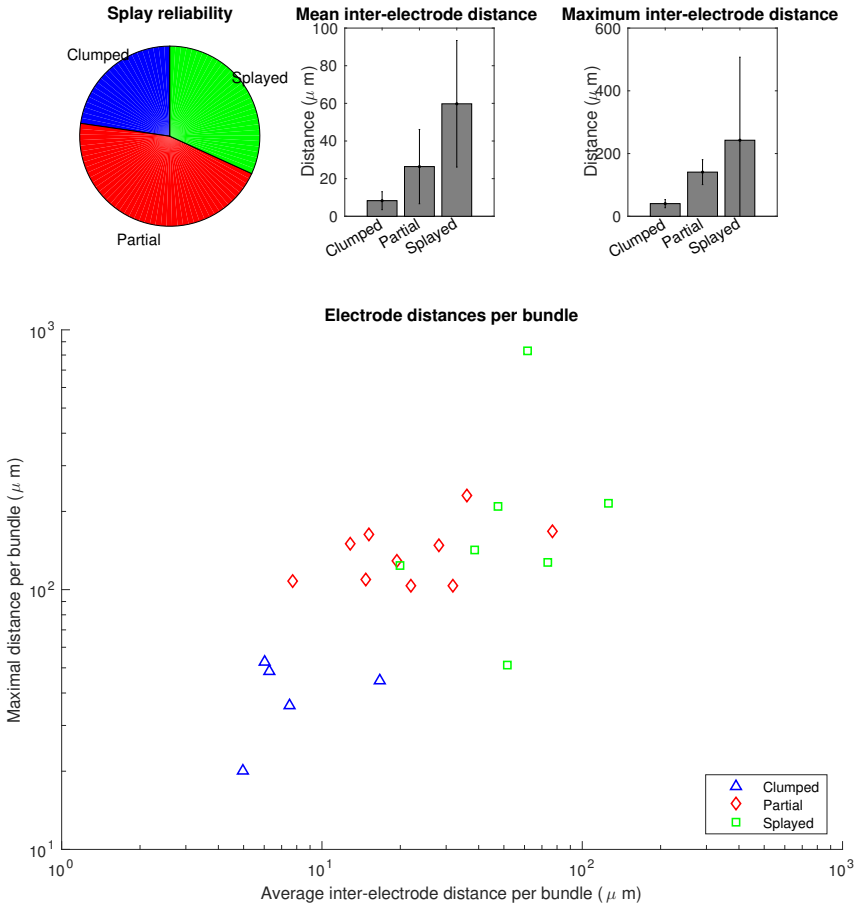

Figure 3. Splay histology data from Table 1.

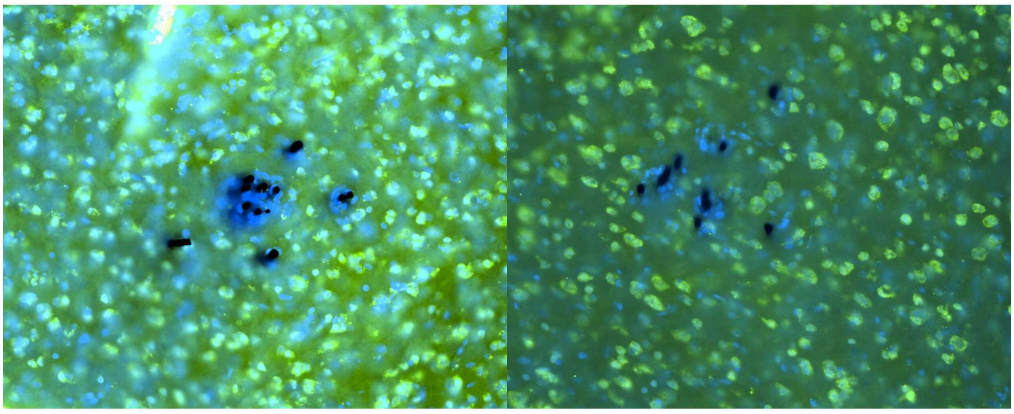

Figure 4. Damage. Neural nuclei are shown in green (stained with NeuN) and all cells in blue (DAPI). The presence of non-neural cells indicates damage, and is notable in the vicinity of the largest non-splayed electrode bundle, and nearly absent around individual electrodes.

I don't have recording-only data from early on.

year. Fig. 5 shows recordings in the weeks leading up to the 1-year mark. These are the three most stable electrodes of the 16.

3.3 Stimulation

Minimising stimulation voltage Some CSCs were better at triggering an antidromic response than others. From the 2^{11} possible CSCs we chose 32 (30 randomly, and the two that treated all electrodes identically). For each CSC, we performed a threshold scan to find the minimum current needed to trigger a response. When this current was found, we performed a voltage scan to find the maximum potential on any electrode. We tested each CSC five times on an anesthetised bird. Results are shown in Fig. 6. The best CSCs resulted in a maximum voltage of around 1 V, while the worst were over 2.5 V. Each threshold scan terminated when a stimulation voltage over 3 V was detected, so we were unable to acquire all five measurements for some CSCs, and thus they are worse than the figure shows. Perhaps surprisingly, the CSCs that sent identical pulses to all 11 electrodes were among the worst performers, with our simple search revealing CSCs that kept voltages far lower.

Controlling the antidromic response

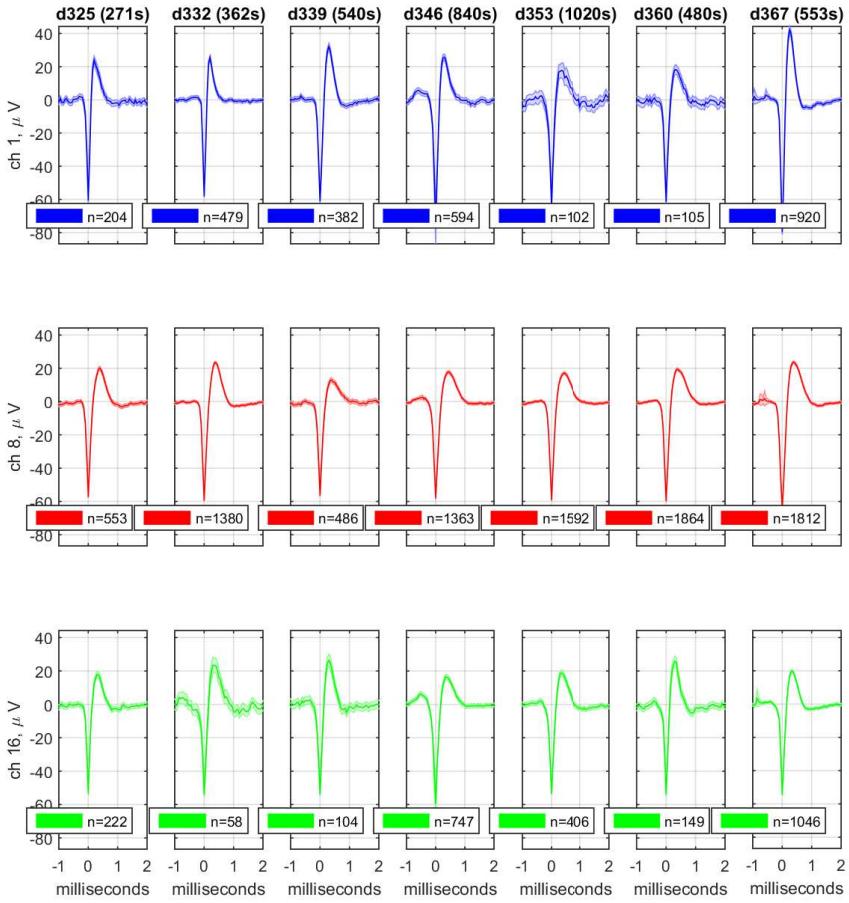

Figure 5. Some of the electrodes in Area X record spontaneous spikes a year after implantation. Column titles show the day post-surgery and the number of seconds of recorded data. Each row is one electrode (shown here: only the four best channels of 16). Legends show the number of spikes; shaded region is mean ± 95% confidence.

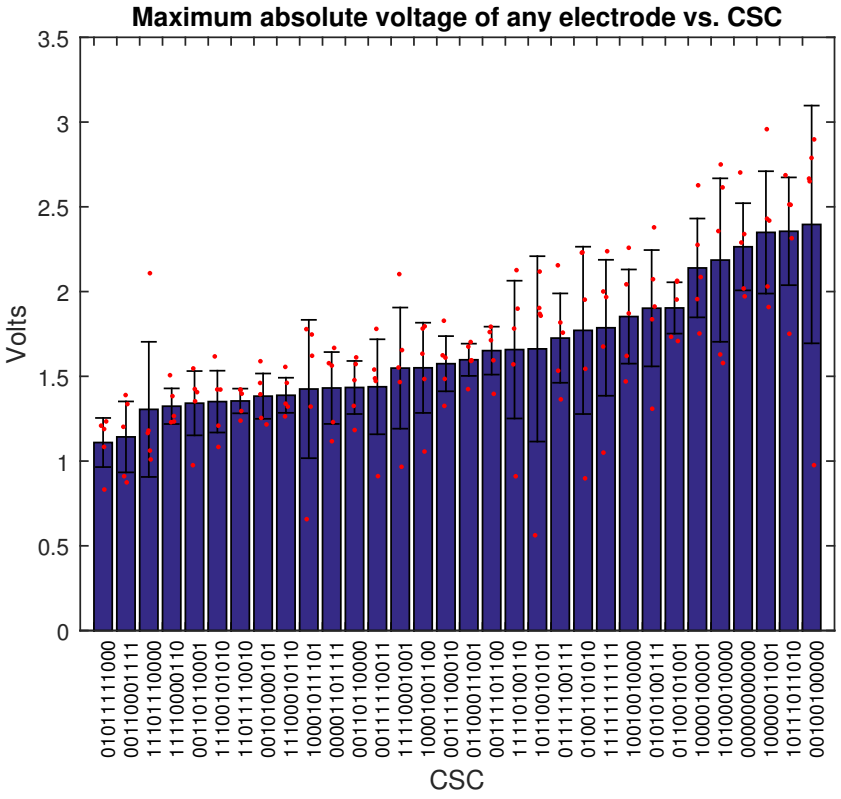

Figure 6. The peak Area X stimulation voltage required in order to achieve biologically effective levels of stimulation in HVC varies with different current-steering configurations. Here are 32 different configurations, over 5 trials each. The X axis lists the configuration (each of the 11 active electrodes delivers a positive-first "0" or negative-first current-controlled pulse "1" pulse). The Y axis shows the maximum voltage across any electrode. Error bars are 95% confidence intervals (n=5), and red dots are the individual trials. For some CSCs, not all trials evoked a response before our 3V threshold was exceeded, and so the true number is higher.

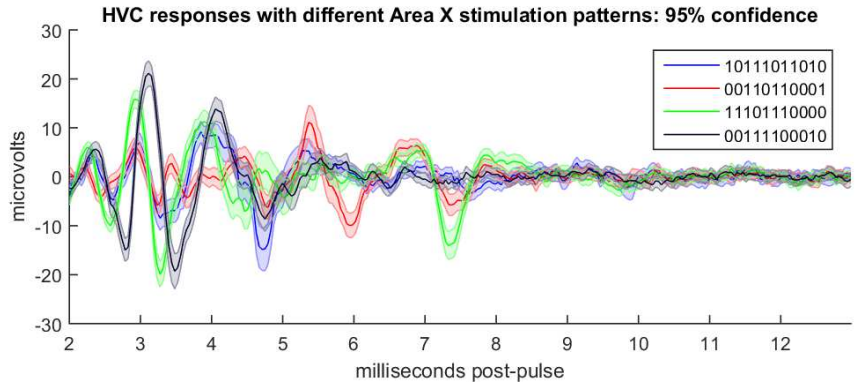

Figure 7. Different CSCs delivered to Area X can induce different responses antidromically in HVC. Here are four of the most distinct responses to four of the 32 CSCs shown in Fig. 6. Shading is 95% confidence, n=198.

4 Discussion

[15] showed that injecting current into tissue causes neurons whose axons are very close to the stimulation site to fire, rather than neurons whose bodies are at greater distances. As a result, the set of neurons that respond to a stimulation pulse is highly sensitive to electrode location, but has spatial extent similar to that of the neuron's dendritic tree. Furthermore, they showed that neurons stimulated in this manner seldom stimulate downstream neurons synaptically.

Splaying electrode arrays with learning stimulation software may be able to exploit these properties. First consider each of the n electrodes in our array separately. n sites stimulated at a given current gives n different random sets of k_n neurons that will fire, and increasing the current changes the size of k. There may exist multiple downstream neurons y such that directly-stimulatable neurons from several of our n sets synapse onto y. This creates a search problem: how to stimulate the n sets in a way that reliably stimulates y enough to cause it to spike? This requires search over current delivered to each group in n in order to control which neurons are recruited, and timing of stimulation delivery to each group in n, so that the downstream neuron is reliably triggered. Different values of current and timing delivered into the n groups may trigger different downstream neurons, so the search problem is: find as many different downstream neurons as possible.

Furthermore, it seems likely that directly-stimulatable neurons may synapse onto others that are directly-stimulatable, once or r times removed. This suggests a further dynamic for the timing search, in which different timings for stimulating the n sets may trigger different firing sequences ([4] proposes a related mechanism in the context of current steering in retina). This enlarges the space of inducible dynamics considerably, and suggests the possibility of inducing Hebbian learning.

Whereas Histed used single electrodes, we use miltichannel arrays. Rather than a 16-channel array providing $n = 16$ groups of neurons, different current-steering configurations may lead to a much higher value of n. For such an electrode there are 2^{16} current-steering configurations even without manipulating current pulse magnitude or timing.

References

1. Holloway KL, Gaede SE, Starr PA, Rosenow JM, Ramakrishnan V, Henderson JM. Frameless stereotaxy using bone fiducial markers for deep brain stimulation. J Neurosurg. 2005;103(3):404–413.

2. Chaturvedia A, Foutza TJ, McIntyre CC. Current steering to activate targeted neural pathways during deep brain stimulation of the subthalamic region. Brain Stimulation. 2012 July;Available from: http://www.sciencedirect.com/science/article/pii/S1935861X11000672.

3. Alexander AL, Lee JE, Lazar M, Field AS. Diffusion Tensor Imaging of the Brain. Neurotherapeutics. 2007 July;4(3):316–329. Available from: http://www.ncbi.nlm.nih.gov/pmc/articles/PMC2041910/.

4. Jepson LH, Hottowy P, Mathieson K, Gunning DE, Dabrowski W, Litke AM, et al.;.

5. Priori A, Foffani G, Rossia L, Marceglia S. Adaptive deep brain stimulation (aDBS) controlled by local field potential oscillations. Experimental Neurology. 2013 July;245:77–86. Available from: http://www.sciencedirect.com/science/article/pii/S0014488612003755.

6. Afshar P, Khambhati A, Stanslaski S, Carlson D, Jensen R, Linde D, et al. A translational platform for prototyping closed-loop neuromodulation systems. Frontiers in Neural Circuits. 2012 January;6(112). Available from: http://www.ncbi.nlm.nih.gov/pmc/articles/PMC3551193/.

7. Rosin B, Slovik M, Mitelman R, Rivlin-Etzion M, Haber SN, Israel Z, et al. Closed-Loop Deep Brain Stimulation Is Superior in Ameliorating Parkinsonism. Neuron. 2011 October;72(2):370–384. Available from: http://www.sciencedirect.com/science/article/pii/S0896627311007768.

8. Biran R TP Martin DC. Neuronal cell loss accompanies the brain tissue response to chronically implanted silicon microelectrode arrays. Experimental Neurology. 2005 September;195(1):115–126. Available from: http://www.ncbi.nlm.nih.gov/pubmed/16045910.

9. VS P, PA T, WM R. Response of brain tissue to chronically implanted neural electrodes. Journal of Neuroscience Methods. 2005 October;148(1):1–18. Available from: http://www.ncbi.nlm.nih.gov/pubmed/16198003.

10. Cogan SF. Neural Stimulation and Recording Electrodes. Annual Review of Biomedical Engineering. 2008;10(1):275–309. PMID: 18429704. Available from: http://dx.doi.org/10.1146/annurev.bioeng.10.061807.160518.

11. Guitchounts G, Markowitz JE, Liberti WA, Gardner TJ. A carbon-fiber electrode array for long-term neural recording. Journal of Neural Engineering. 2013;10(4). Available from: http://www.ncbi.nlm.nih.gov/pmc/articles/PMC3875136/.

12. Swadlow HA. Neocortical efferent neurons with very slowly conducting axons: strategies for reliable antidromic identification. Journal of Neuroscience Methods. 1998 February;79(2):131–141. Available from: http://www.sciencedirect.com/science/article/pii/S0165027097001763#BIB51.

13. Hahnloser RHR, Kozhevnikov AA, Fee MS. An ultra-sparse code underliesthe generation of neural sequences in a songbird. Letters to Nature. 2002 September;419:65–70. Available from: http://www.nature.com/nature/journal/v419/n6902/full/nature00974.html

14. Fee MS, Kozhevnikov AA, Hahnloser RHR. Neural Mechanisms of Vocal Sequence Generation in the Songbird. Ann NY Acad Sci. 2004;1016:153–170. Available from: http://web.mit.edu/feelab/publications/Fee%20et%20al%20NYAS%202004.pdf.

15. Histed MH, Bonin V, Reid RC. Direct activation of sparse, distributed populations of cortical neurons by electrical microstimulation. Neuron. 2009 August;63(4):508–522. Available from: http://www.ncbi.nlm.nih.gov/pmc/articles/PMC2874753/.